Suv420 Localization During Mitosis is Regulated by Phosphorylation

A Major Qualifying Project

submitted to the Faculty of

WORCESTER POLYTECHNIC INSTITUTE

In partial fulfillment of the requirements for the

degree of Bachelor of Science in Biology and Biotechnology

by

Hannah Shell

Date:

27 April, 2023

Report Submitted to:

Amity Manning, PhD

Worcester Polytechnic Institute

Table of Contents

Acknowledgements

I would like to thank the entire Manning Lab at Worcester Polytechnic Institute, but I would especially like to thank my MQP advisor Professor Amity Manning, our lab advisor Nicole Hermance, and graduate students Sabine Hahn, Elizabeth Crowley, Greg Zamalloa and Weikang Fu for guiding me in my research.

Abstract

Experimental manipulation of localization of the methyltransferase Suv420 at centromeres suggests that proper localization of Suv420, or its placed epigenetic marks, are critical for correct chromosome segregation during mitosis. It is suggested that it does this by indirectly regulating kinetochore-microtubule attachment. However, it remains unknown how discrete Suv420 localization to pericentromeres, and not centromeres, is achieved. Analysis of Suv420's amino acid sequence in software to identify potential protein binding domains that are near mutations relevant to cancer predict four residues that may be phosphorylated by mitotic kinase Nek2. Nek2 inhibition and phosphatase inhibition of mitotically arrested retinal pigment epithelial cells containing doxycycline-induced Halo-tagged Suv420 plasmids confirm that Suv420 localization to pericentromeric chromatin during mitosis is regulated by phosphorylation. However, neither phosphomimetic mutations of Serine 20 nor Serine 355 on Suv420 were found to significantly change Suv420 localization, suggesting further tests with different Suv420 mutations and combinations of mutations is needed.

Introduction

Cancer - A Disease Caused by Misregulation of the Cell Cycle

From 2013 to 2017, the United States national overall cancer incidence rates (diagnosis in a population of 100,000) for all ages were found to be 487.4 among males and 422.4 among females [Islami et al., 2021]. It is estimated that in the United States in 2022, close to 2 million people will be diagnosed with cancer and over 600,000 of those people will die of it [Bethesda, 2022]. As research has progressed, scientists have concluded that cancer is the result of individual cells of the body escaping the normal pacing and control of the cell cycle due to an accumulation of key genetic mutations that result in toxic cell replication and overgrowth [Bethesda, 2022; Ong & Torres, 2019]. Normally, cells are tightly regulated by an intricate set of checks and balances to control exactly when, how and where a cell will undergo growth and division, a process known as the cell cycle. However, cancer can occur when the activity of proteins directly responsible for catalyzing or inhibiting continuation in the cycle are perturbed [Cooper, 2000].

The cell cycle can be divided into four phases: Gap 1 (G1), DNA replication/synthesis (S), and Gap2 (G2), and mitosis (M). Within each phase are also multiple checkpoints with distinctive molecular interactions that stop to verify that the intracellular and extracellular conditions are sufficient for the cell to continue the cycle. There are a total of 4 major checkpoints, the G1/S checkpoint, the intra-S phase checkpoint, the G2/M checkpoint, and the Spindle Assembly checkpoint (Figure 1A) [McIntosh, 2016; Bethesda, 2022]. The cell cycle begins with cell growth in which the cell gathers nutrients. In a multicellular organism, cells that are in a fully differentiated state perform their primary function as part of whatever tissue's stem or progenitor cells it was generated from. For many cells of the body, completed differentiation will often mean that they will not divide again and will instead continue to perform their primary function until death. Such determination regarding whether a cell will pass G1 or not is determined at the G1/S checkpoint. The G1/S checkpoint, in addition to checking for DNA damage, is the catalyst of division, determining whether the cell will remain in a senescent state, or if it will enter the irreversible process of replication and division. If a cell passes G1 checkpoint, it is then committed and will continue to divide regardless of the changing signals from outside.

Cells that continue in the cycle next replicate their genetic code during S phase until it reaches the intra-S phase checkpoint to check for DNA damage and errors in DNA replication. If

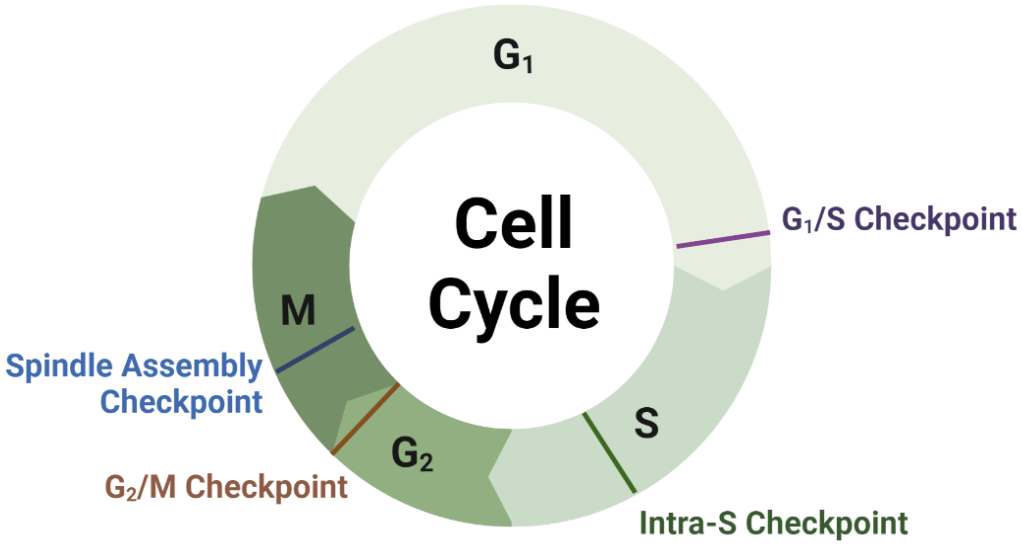

A.

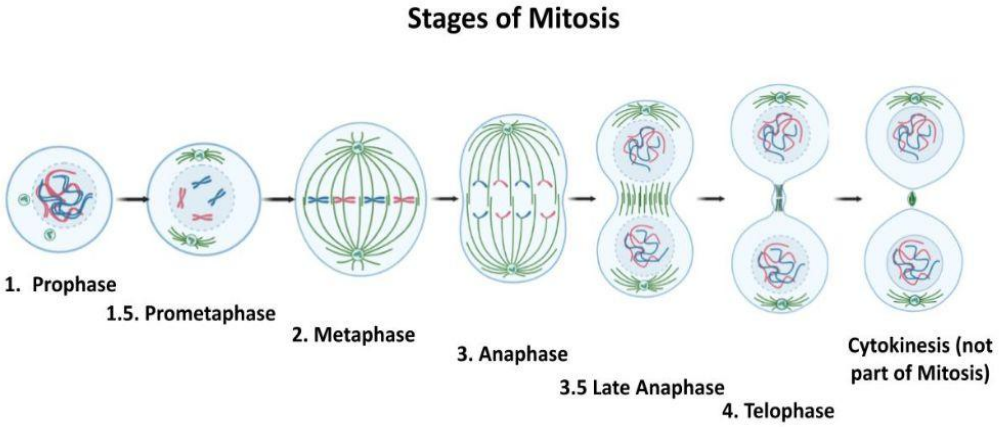

B.

Figure 1: Overview of the Cell Cycle and Mitosis

A. The cell cycle consists of four main phases: Gap 1 (G_1), Synthesis (S), Gap 2 (G_2) and Mitosis (M). Within each phase also exists four major checkpoints that assess whether the cell should continue through cell division: G_1/S checkpoint, Intra-S checkpoint, G_2/M checkpoint, and the Spindle Assembly Checkpoint. Image created using Biorender.com

B. Mitosis consists of four continuous phases: Prophase, Anaphase, Metaphase and Telophase. Mitosis is then concluded with the beginning of cytokinesis. Image created using Biorender.com

only some damage is present or minor errors have occurred, the cell will attempt to repair these sites and edit the errors it is able to find to allow the cell to continue division, but if the damage is too great or too many major errors were made, the cell is programmed to undergo apoptosis [Cooper, 2000]. After the cell has verified that it has correctly replicated its DNA and all detected damage or errors have been correct, the cell approaches the second Gap phase (G2), during which it prepares for division by continuing to gather more materials and nutrients to build enough cell mass for two individual cells [Albert et al., 2002].

Eventually, the cell reaches the G2/M checkpoint, where it will once again verify that it has successfully accumulated sufficient cell mass and that each copy of its replicated DNA remains undamaged and is without error. If the cell passes this checkpoint, it can finally undergo mitosis, a process that can be divided into 4 continuous phases (Figure 1b). The first is prophase, where the cell condenses its DNA into chromosome pairs called sister chromatids while centrioles that were duplicated in G2 now move towards opposite sides of the cell. The second step, an intermediary but distinct step between two phases, is prometaphase, where microtubules then polymerize outwards from the centrioles to form the mitotic spindle and attach to the chromatids at a special protein complex called the kinetochore, which assembles at a specific region of heterochromatin on the chromosome called the centromere (represented in Figure 2 below) [McIntosh, 2016]. Microtubules can then both grow and depolymerize while maintaining stable association with kinetochores during metaphase to then bring each sister chromatid pair to the center of the cell as attachment from each microtubule increasingly stabilizes. It is the association of a kinetochore/chromosome with a shrinking microtubule that drives chromosome movement towards the spindle pole. When chromatid pairs become amphitelically attached such that the kinetochore on each chromatid is associated with microtubules emanating from an opposite spindle pole, the forces exerted by depolymerizing microtubules are balanced and the chromosome aligns at the center of the cell. Once all chromosomes have achieved amphitelic attachment and have aligned at the center of the cell, the cell is said to be in metaphase. It is now that the cell has arrived at the final major cell cycle checkpoint, the Spindle Assembly checkpoint. Here, the cell verifies stable connection between the chromosome's kinetochores and their attached microtubules, as well as sensing interkinetochore tension between sister chromatids that are being pulled on by opposing centrosomes at the cell's poles. Once the chromosomes have been aligned along the spindle equator in a bipolar fashion, the activity of the spindle assembly checkpoint protein complex becomes down regulated and the anaphase-promoting complex/cyclosome is allowed to cut the cohesin protein keeping the sister chromatids together. In this way, the spindle assembly checkpoint verifies that all the chromosomes are properly aligned at the spindle equator so that when they're finally pulled apart towards each centriole by shortening mitotic spindle fibers in anaphase, each daughter cell will have a complete, undamaged copy of the parent cell's DNA [Musacchio & Salmon, 2007; McIntosh, 2016]. After passing through anaphase, the cell enters telophase, where a new nuclear membrane forms around the recently divided chromosomes that begin to decondense back into chromatin to create two new daughter nuclei. Telophase is then followed by cytokinesis that segregates the cell's cytoplasmic components in half with a newly formed cell membrane, completing the final step of the cycle and allowing the new daughter cells to reenter the growth phase [McIntosh, 2016].

In cancers, it is often found that major proteins/genes involved in regulation of each cell cycle checkpoint are mutated or epigenetically altered in some way to permit the cell to undergo division regardless of the internal or external conditions, and without regard to the presence of significant DNA damage. Changes to the expression of these genes allow the cell to bypass the

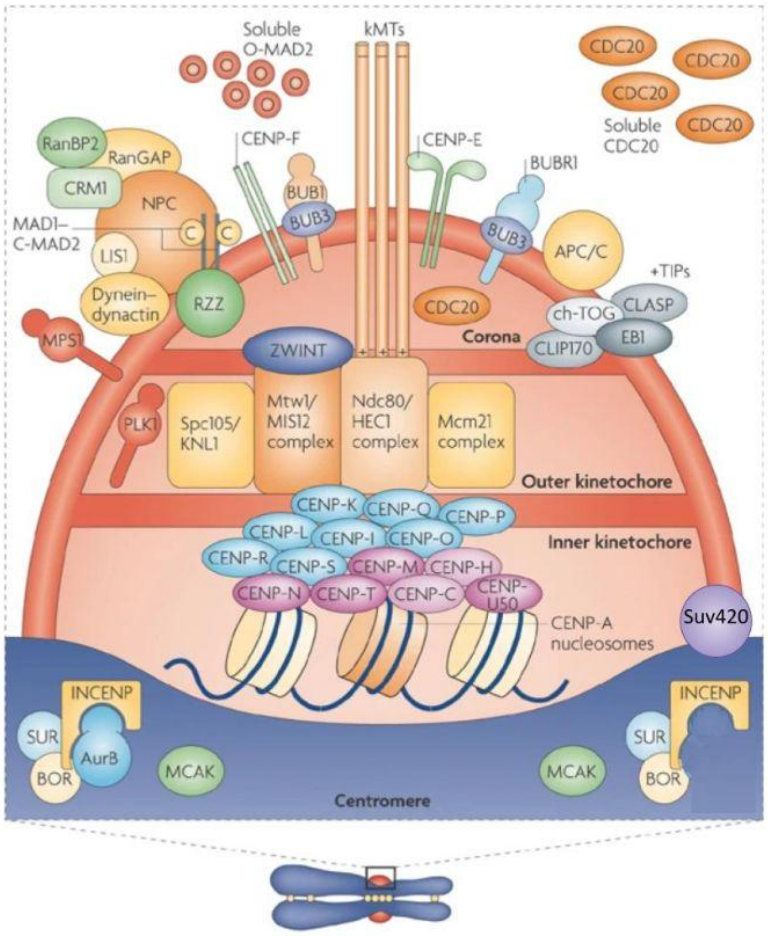

Figure 2: Protein Interactions Regulating Microtubule-Kinetochore Attachment

Above is a visual representation of the many proteins involved in regulating microtubule-kinetochore attachment during mitosis, adapted from Figure 4 of Musacchio & Salmon [2007]. As seen, Suv420 sits just outside the centromere of the chromosome (at the pericentromere), but does not allow for Aurora B localization to the centromere when Suv420 is present.

checkpoints and enter the next stage of division without ensuring correct genetic replication and segregation. A few well-known proteins that become mutated or epigenetically altered and contribute to cancer development include pRb [Sachdeva & O'Brien, 2012], a major regulator at the G1 checkpoint that inactivates transcription factor E2F to prevent cellular entry into S phase [Herwig & Strauss, 1997], and p53 [Hu et al, 2021] that regulates the G1, intra-S phase and G2/M checkpoints to monitor for DNA damage. Each gene discovered to contribute to the development of cancer when mutated or epigenetically altered is categorized into two classes based on their normal role within the cell and the resulting phenotype when a change in their activity occurs. The two classes are oncogenes that over promotes cellular growth and division when abnormally activated or overexpressed, and tumor suppressor genes, such as pRB and p53, that promote cellular growth and division when inhibited or silenced [Chow, 2010] .

Like a variety of genes at the G1/S, intra-S phase and G2/M checkpoints, misregulation of many genes found at the Spindle Assembly checkpoint have been associated with a number of cancers and potential cancer therapies [Curtis et al., 2020], making it an ideal subject for many cancer studies. As previously mentioned, the spindle assembly checkpoint checks for stable kinetochore/chromatin attachment during mitosis. The mitotic spindle must bind in a stable manner to the centromere of each chromosome via the kinetochore to be able to pull it into alignment at the spindle equator for division. However, both the mitotic spindle and the kinetochore are dynamic structures and do not simply chemically bind permanently to the centromere. The mitotic spindle is made up of multiple tubulin filaments that are constantly shortening and lengthening (by adding or removing tubulin dimers) in a process called dynamic instability. The removal and adding of tubulin filaments occurs adjacent to the kinetochores, where the tubulin dimers are constantly disassociating unless they're stopped by various proteins present at the centromere [McIntosh, 20216; Musacchio & Desai, 2017; Hinshaw & Harrison, 2018]. Failure to regulate this dynamic instability correctly leads to misalignment and improper segregation of chromosomes (whether entire chromosomes are pulled in the wrong direction or chromosomes are ripped apart and segregated in pieces). This in turn can lead to such severe genetic alteration that the daughter cells are often nonviable [Cooper, 2000]. However, cells that do survive missing one or more chromosomes, or acquire extra chromosomes (called aneuploidy) often result in significant phenotypic change at both the cellular and organismal levels from the genetic and proteome imbalance. Such changes may include abnormal growth and division rates of cells that can result in impairment of vital organs from excess growth, as seen in both cancer that can be highly aneuploid [Gordon et al., 2012; Taylor et al., 2019]]. It should be noted however, that based on the missegregation error that occurs and which genes are altered, aneuploidy can rear a double head to promote tumorigenesis and also fight it, found to exert substantial tumor suppressive effects by deleting critical growth genes still required by cancer cells to grow, making aneuploidy a critical topic of many cancer studies [Taylor et al., 2019; Vasudevan et al., 2021], including this project.

Aurora B - Regulating Kinetochore-Microtubule Attachment in Mitosis

One critical protein that has been found to be involved in spindle assembly checkpoint regulation is mitotic kinase Aurora B (referred to AurB in Figure 2 above) [Herlihy et al, 2021; Broad et al, 2020]. Aurora B kinase has been found to regulate kinetochore and spindle attachment by varying its localized concentrations to control the attachment and detachment of the mitotic spindle fibers to the kinetochores. It was found that early in mitosis, kinetochores undergo repeated cycles of attachment and detachment that are catalyzed by Aurora B dependent phosphorylation of protein Hec1/Ndc80 (a member of the NDC80 complex within the kinetochore at its interface) [Ciferri et al., 2005; Welburn et al., 2011; Hindriksen et al., 2017; Broad et al. 2020; Liang et al., 2020]. Aurora B, along with three other proteins INCEP, Survivin/BIRC5, and Borealin/CDCA8, form the chromosomal passenger complex (CPC) that localizes from the chromosomal arms to the centromere during early mitosis. Aurora B

localization to the centromere promotes loading of cohesin I and phosphorylation of various substrates including Histone 3, stathmin, mitotic centromere-associated kinesin, & Hec1 to stabilize and destabilize microtubule- kinetochore attachment. This continuous stabilization and destabilization is done to prevent the microtubules from incorrectly attaching and accumulating incorrect attachments. However, as mitosis progresses and the chromosomes are pulled to the spindle equator, the kinetochore-spindle fiber attachments become increasingly stable, with Aurora B activity continually decreasing as the outer interface of the kinetochore is pulled away from the centromere, no longer able to interact with Aurora B. This mechanism ultimately also allows Aurora B to play a critical role in correction of attachment errors and regulation of the spindle assembly checkpoint with the recruitment of checkpoint protein BUBR1 that promotes association to the anaphase promoting complex/cyclosome [Ruchaud et al., 2007; Welburn et al., 2011; Hindriksen et al., 2017; Broad et al, 2020]. Other studies also support this proposed mechanism by finding that loss or functional inactivation of Aurora B kinase activity prevents correction of mitotic spindle attachment and leads to corruption of correct mitotic segregation [Lamson et al., 2004; Liang et al., 2020], making Aurora B a key protein involved in catalyzing continuation of cell division at the final major checkpoint of the cell cycle.

Aurora B Localization is Epigenetically Regulated by Suv420H2

After discovering that Aurora B was the key protein in determining correct mitotic spindle attachment, the next question to be posed was to find out what key protein was controlling Aurora B. Separate studies had already discovered that epigenetic methylation of specific histones found in the heterochromatin at (centromeric) and near (pericentromeric - less ordered repeat sequences flanking centromeric chromatin containing histone CENP-A [Ruchaud et al., 2007]) the centromere of chromosomes during mitosis also significantly impacts genomic stability and metastatic potential of many various cancers. Most specifically, it has been found that increased localization of methyltransferases Suv39 and Suv420 (whose variants methylate pericentromeric enriched histones H3K9me2/3 and H4K20me2/3) at the centromere strongly correlated with increased mitotic segregation errors and thus also aneuploidy [Janssen et al., 2018; Zhou et al., 2019 Herlihy et al., 2021]. In addition to two other known CPC localization signaling pathways involving histone kinases Haspin (which phosphorylates histone 3 on threonine 3 - H3T3) and Bub1 (which phosphorylates histone 2 at threonine 120 - H2AT120) [Hindriksen et al., 2017; Hadders et al., 2020], it had thus been hypothesized that methylation regulation at the pericentromere may also impact Aurora B localization to the centromeres.

Herlihy et al. confirmed that increased localization of both Suv39 and Suv420H2 to the centromere both suppressed centromere transcription and inhibited Aurora B kinase localization to the centromere (as represented on the bottom right side of Figure 2 above), thus allowing for increased stabilized incorrect microtubule attachment to kinetochores and therefore compromising mitotic segregation fidelity. Additionally, they also found that inhibition of Suv420 activity specifically led to improved mitotic segregation by partially restoring Aurora B

and CPC localization to the centromere, and that upregulation of Suv39 and Suv420 expression corresponded with significantly increased sensitivity to five of six tested Aurora B kinase specific inhibitors in cancer cells. However, despite confirmation that Aurora B localization to the centromere is likely negatively regulated in some way by Suv420, the possibility that this regulation is independent of Suv420's methyltransferase activity does exist. Regardless of this though, the question following these findings then becomes what regulates Suv420, which is to be investigated by this project.

Motif Interaction Software Predicts Four Nek2 Phosphorylation Sites on Suv420

Suv420 is one of many protein lysine methyltransferases (PKMTs) that plays an active role in cell cycle regulation by participating in chromatin assembly, DNA replication, DNA damage response and repair, and mitotic chromosome segregation fidelity [Bromberg et al., 2017; Southall et al., 2014; Wang et al., 2018]. As previously mentioned, Suv420's target substrate of methylation is the twentieth lysine on histone 4 (H4K20) (represented below in Figure 3)that has already been methylated at least once (H4K20me1) by a different methyltransferase, PR-SET7. Suv420 adds at least the second methyl group to H4K20me1, creating H4K20me2 [Bromberg et al., 2017]. Although H4K20me2/3 have been found to be enriched at the pericentromere [Herlihy et al. 2021], globally, H4 is found 90% of the time to be dimethylated at lysine-20, making it one of the most prevalent marks in the genome [Southall et al., 2014], likely due to its role in sensing DNA damage. Multiple studies have found that direct

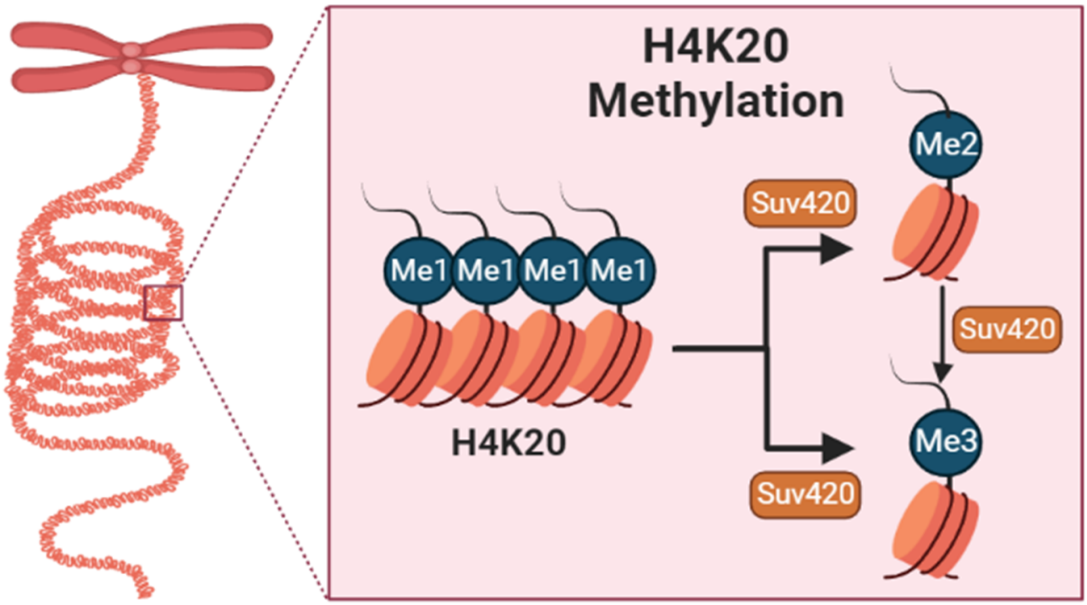

Figure 3: Suv420 Dimethylates H4 at Lysine 20 on Chromosomes
Methylation of Lysine 20 on Histone 4 catalyzed by methyltransferase Suv420 is shown above. Methylation occurs during mitosis, when the cell's DNA has been compacted into chromosomes [Bromberg et al., 2017; Wang et al., 2018]. Image created in Biorender.com

and preferential binding of H4K20me2 by p53-binding protein 1 (53BP1) links it to signaling in double-stranded DNA break repair through recruitment of Orc1 protein, which is required to pass the intra-S phase checkpoint in the cell cycle[Southall et al., 2014; Bromberg et al., 2017; Gupta et al, 2014]. Trimethylated H4K20 has been found to be linked with epigenetic transcriptional regulation, where H4K20me3 actively silences specific genes. It should be noted that a conclusion on what trimethylates H4K20 during epigenetic silencing is still unknown and research indicates that it is likely not Suv420 performing the trimethylation[Wang et al, 2018; Herlihy et al. 2021], however Suv420 knock down in leukemia cells has still been found induce G1 arrest at the G1/S checkpoint by allowing for re-establishment of active transcription of tumor suppressor p21, which had been previously silenced by Suv420 [Wu et al., 2018; Shamloo & Usluer, 2019]. This implies that although Suv420 may not be directly methylating and silencing tumor suppressors, it still plays a key role in that process, where it is required in the pathway and thus still a potent target for cancer therapeutics [Wu et al., 2018; Shamloo & Usluer, 2019].

Given Suv420's critical roles in regulating cell cycle progression, this then raises the next question of what regulates Suv420. What cellular mechanism directs it to localize near its H4K20me2/3 targets at the pericentromere during specific phases of the cell cycle and what inactivates it to allow for Aurora B localization during anaphase? This can be hypothesized by looking at the linear amino acid sequence of Suv420 and running this sequence through a variety of protein databases. The first database would be one that identifies protein motifs and binding domains found on Suv420 that may act as potential binding sites of other proteins in the human genome, which can be done using a number of online databases [Mulder & Apweiler, 2002]. However, doing so can generate a long list of potential target sequences on Suv240, so to search the next database to run the sequence through would be one identifying those same binding interactions but further identifying interactions that are nearby mutations relevant to cancer. One such software capable of this task is the 2022 release of the Eukaryotic Linear Motif Resource for Functional Sites in Proteins (ELM) by Kumar et al. [2021].

One such protein that serves as a strong candidate that potentially phosphorylates Suv420 at 4 potential sites is the never-in-mitosis-gene-A-related-kinase-2 (Nek2). Nek2 is a mitotic serine/threonine kinase that has been found to play critical roles in centrosome separation, chromatin condensation and segregation, kinetochore attachment, microtubule stabilization, and regulation of the spindle assembly checkpoint of the cell cycle. Regulated by CDK4, MST2 and p90RSK2 (an effector of mitogen activated protein kinase MAPK - activates NEK2 catalytic domain via phosphorylation), upregulation of Nek2 expression has been found in a large variety of human cancers, altering the precise balanced activity of a large number of critical proteins within the cell. These include β-catenin, rootletin, Nlp2, Hec1, MAD2, and HMGA2, and alteration of these proteins activity generally results in aneuploidy, instability, premature chromosome segregation and instability, and ultimately abnormal proliferation of cells [Shah et al, 2022]. Particular attention has been drawn in recent years to Nek2's oncogenic role in activating the Wnt/β-catenin signaling pathway via activation of AKT/Protein kinase B (PKB)

[Shah et al, 2022; Xie & Weiskirchen, 2020] and inactivating the Hippo pathway via cooperation with the STRIPAK complex to promote expression of connective tissue growth factor (CTGF), cysteine-rich heparin-binding-protein 61 (CYR61) and glioma-associated oncogene family zinc finger2 (GLI2) in cervical cancer [Shah et al, 2022; Zhang & Zheng, 2022]. Given Nek2's localization to the centromeres specifically earlier in mitosis, its critical role in kinetochore attachment and chromosomal segregation, having multiple potential phosphorylation sites on Suv420, it has been concluded to be a strong candidate of Suv420 regulation during mitosis. This project thus aims to investigate and test this relationship to better understand Suv420 roles in mitotic fidelity regulation and in cancer development, progression and treatment.

Methodology

In order to determine if there exists a causation relationship between Nek2 and Suv420 localization to chromatin during mitosis, the first step of this project looked into testing whether inhibition of Nek2 or overactivation of Nek2's phosphatase activity affected Suv420's location within the cell during mitosis. This was done by treating retinal pigment epithelium (RPE) cells previously transformed with a doxycycline-inducible plasmid containing a Halo-tagged wild type Suv420 gene and with mitosis arresting drug nocodazole [Beswick et al., 2006] for 18 hours and adding Nek2 inhibitor drug Rac-CCT (Nek2i) [Innocenti et al., 2012] or phosphatase inhibitor calyculin A (CalcA) [Ishihara et al., 1989], performing small scale fractionation to separate the cellular proteins into chromatin-bound proteins and all other cellular proteins (soluble cytoplasmic and nucleoplasmic proteins). Gel electrophoresis and western blotting was then performed to separate all cellular components by size and ImageJ of the blots was used to quantify relative amounts of four proteins: the Halo-tagged wild type Suv420, known cytoplasmic proteins glyceraldehyde 3-phosphate dehydrogenase (GAPDH) and alpha tubulin (dm1α-T) [Zhang et al., 2015; Binarová & Tuszynski, 2019], and known chromatin-bound protein Histone 3 (H3) [Shi et al., 2017].

After confirmation that Nek2 inhibition and overactivation significantly impacted Suv420 localization to chromatin during mitosis, four potential sites of Nek2 phosphorylation of Suv420 were identified as relevant to cancer by running the nucleotide sequence of Suv420 through Kumar et al.'s ELM database (2021) (see Figure 4 below). The first site identified was a serine

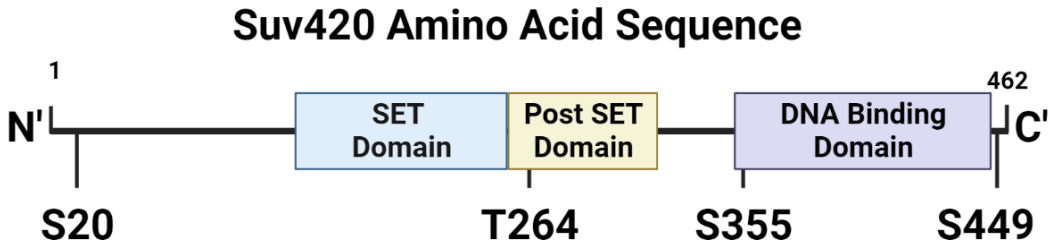

Figure 4: Suv420 Amino Acid Sequence with Identified Nek2 Phosphorylation Sites
Kumar et al.'s [2021] ELM database identified four potential Nek2 phosphorylation sites on Suv420 near cancer relevant mutations that may potentially disrupt kinase binding. All four predicted residues fall outside of Suv420's set domain.

residue at position 20 (S20). In order to determine if this site impacted Nek2 phosphorylation of Suv420, S20 on the wild type, Halo-tagged Suv420 plasmid was mutated to an alanine (S20A) and an aspartic acid (S20D) to reflect inhibition and overactivation of phosphorylation respectively. Each plasmid (Suv420-S20A and Suv420-S20D) were then transformed into new RPE cell lines. Small scale fractionation of mitotic cells, gel electrophoresis, Western blotting and ImageJ analysis were repeated for the new mutants alongside wild type Suv420-Halo cells.

Following identification of four potential Nek2 phosphorylation sites on Suv420 using the ELM resource [Kumar et al., 2021], the second site that was tested was the 355th serine

residue (S355). Once again, to model inhibition and overactivation of Nek2 phosphorylating Suv420, the S355 was mutated to an alanine (S355A) and aspartic acid (S355D). Small scale fractionation of mitotic cells, gel electrophoresis, Western blotting and ImageJ analysis were repeated again alongside wild type Suv420-Halo cells. All material concentrations, company names and catalog numbers are listed below in Table 1.

Transformation of RPE tetR Suv420-Halo Cell Lines

Transformation of the retinal pigment epithelial (RPE) cell lines with a tetracycline inducible Halo-tagged Suv420 expression construct was performed by Nicole Hermance from Dr. Amity Manning's Lab. Primers for Suv420 were designed by first identifying both the wild type sequence of Suv420 (KMT5C) and the putative Nek2 phosphorylation sites to be mutated on the sequence (in this case, Serine 20 and Serine 355). Codons for each specific amino acid were identified and primers were then designed based on the mutation required to change the amino acid from serine to either alanine or aspartic acid. Four total PCR reaction mixtures were then created containing pucGW plasmids with DNA primers to generate Suv420-Halo S20A, Suv420-Halo S20D, Suv420-Halo S355A, or Suv420-Halo S355D mutations from the cDNA of the wild type Suv420 gene. The PCR reactions were run for 26 cycles and plasmid size was verified by DNA gel electrophoresis. A ligation reaction was then performed using DpN1, 5x ligation buffer and T4 DNA Ligase, and resulting digested ligation reaction mixtures were used to perform transformation of DH10B competent *E. coli* cells incubated in kanamycin for vector propagation of the Suv420 containing vector. Gateway vector cloning as outlined by Invitrogen Life Technologies [Invitrogen, 2023] was then performed to add the Halo tag to the C' terminus of Suv420's sequence and place Suv420-Halo into a tetracycline inducible lentiviral puro-resistant destination vector. These vectors are then used to transform 293T cells to create viruses whose supernatant was used to then transfect each of the five RPE cell lines.

Small Scale Fractionation

Small scale fraction was performed in four stages. The first was seeding and incubation of RPE cell lines, followed by doxycycline and nocodazole treatment, then Nek2i and CalcA treatment, and finally fractionation. The RPE cell lines used were immortalized cells previously transformed with a plasmid containing various mutations of a Halo-tagged human Suv420h2 gene under the control of a tetracycline regulator (tetR with doxycycline being the tetracycline of choice for regulation). Received cell lines frozen in 10% dmso and filtered Dulbecco's Modified Eagle's Medium (dmem) containing penicillin-streptomycin (penstrep) and fetal bovine serum (FBS) (445mL dmem, 50mL FBS & 5mL penstrep) were thawed and plated on sterile $10cm^2$ tissue culture dishes under a sterile tissue culture hood, and stored in a 37ºC incubator for 24 hours. After 24 hours, old media and dead cells were removed and new media was added, and the plates were placed back into the 37ºC incubator. Once the plates reached at least 75% confluency (roughly another 24-48 hours later), the cell lines were split 1:5, with 2mL of 10mL of trypsin (inactivated by the growth media), dmem growth media and cells transferred to a new

$10cm^2$ tissue culture plate, followed by 8mL of growth media and storage in in the 37ºC incubator for another 48-72 hours (until 75% plate confluidity). For the second division, in addition to the splitting and continual division of the cell lines, 3mL of cells/media/trypsin were also transferred to varying numbers of sterile T-75 flasks based on the conditions of the experiment. During initial protocol optimization and verification of Nek2 influence on Suv420 localization, the cell line containing the wild type Halo-tagged Suv420 (WT) was distributed into three T-75 flasks in addition to a $10cm^2$ plate to continue the cell line. Once the mutants were introduced, the WT line was distributed into two T-75 flasks and all mutant versions of Suv420-Halo (Suv420-Halo S20A, Suv420-Halo S20D, Suv420-Halo S355A and Suv420-Halo S335D) were distributed to only one T-75 flask in addition to a new $10cm^2$ plate to continue each cell line.

The second stage of small scale fractionation was doxycycline and nocodazole treatment to induce Suv420-Halo expression and induce mitotic arrest respectively. All of the T-75 flasks for each experiment were all allowed to incubate at 37ºC for 24 hours before 10µL of 2mg/mL doxycycline was added to each T-75 flask (referred to as +D). The only T-75 flask that did not receive doxycycline was the third T-75 of the optimization and verification experiment for all performed replicates, which allowed for verification that the doxycycline was directly causing the expression of the Suv420-Halo. 6 hours after addition of doxycycline, 10µL of 10µg/mL nocodazole (from a 1:100 stock of 10mg/mL suspended in dmso) was added to every T-75 flask to induce mitotic arrest for an 18 hour period (referred to +Noc).

The third stage of small scale fractionation was mitotic cell shake off and treatment of two WT lines with either Nek2 inhibitor or calyculin A. 18 hours after addition of nocodazole, all of the T-75 flasks underwent mitotic shake off to suspend only mitotic arrested cells in the cell media that was then collected and kept in suspension in 15mL conicals. A cell count of every cell line was then conducted and the volumes within each conical was balanced to ensure that the concentration of cells in each condition was the same. The WT +D/+Noc cells were combined during counting and then divided into three 15mL conicals. Two of these conicals then received 10µL of 10mM Nek2i or 10µL of 100mM CalcA. Nek2i inhibits Nek2 by binding to its catalytic pocket to prevent phosphorylation [Innocenti et al., 2012] while CalcA inhibits general dephosphorylation across the cell as a phosphatase inhibitor [Ishihara et al., 1989]. All the 15mL conicals were then placed back in the 37ºC incubator for 1 hour.

The final stage of small scale cell fractionation was fractionation itself to produce samples containing all proteins within the cell (whole cell lysates - WCL), only chromatin-bound proteins within the cell (CB), and only soluble cytoplasmic and nucleoplasmic proteins within the cell (S). 500mL of cells were removed from each of the 15mL conicals for whole cell lysis fractions. These cells were isolated from the cell media vai centrifugation (2000rpm for 5 minutes) and resuspended in 35µL of 4X Laemmli sample lysis buffer diluted to 1X in hypotonic sample lysis buffer. The remaining cells from the 15mL conicals were also isolated from the cell media via centrifugation and decantation (3000rpm for 5 minutes), followed by a warm PBS wash (5mL, 1X PBS), a second centrifugation and decantation (3000rpm for 5 minutes), and

finally a cold PBS wash (5mL, 1X PBS cooled on ice for 15 minutes) with a third centrifugation and decantation (3000rpm for 5 minutes). The cells of each conical were then resuspended in 50µL of hypotonic buffer, transferred to labeled 1.5mL microfuge tubes, and placed on ice for 15 minutes to prepare the cells for lysis. Lysis was performed by very quickly adding 3.13µL of 10% NP40 to the chilled cells and rotating them at 4°C for another 15 minutes. To ensure proper lysis, addition of 10% NP40 and placement on a rotator was done one immediately after the other for each sample, rather than adding the NP40 to all samples and then placing all the samples on the rotator. The chromatin-bound proteins were then separated from soluble proteins by centrifugation (13000rpm for 5 minute) at 4°C and the supernatant was transferred to newly labeled microfuge tubes with 17.71µL of 4X sample lysis buffer. Chromatin-bound protein pellets were then resuspended in 70.84µL of 1X hypotonic sample lysis buffer and all microfuge tubes for soluble and chromatin-bound protein were boiled for 5 minutes at 95°C and stored at -20°C. It should be noted that once the mutant Suv420-Halo cells were included in the samples, all centrifugation times were changed to 8 minutes to improve separation of supernatant and pellets.

Gel Electrophoresis, Western Blotting and Autoradiography

A total of 4 (two 10%, 15-well and two 15%, 15-well) polyacrylamide gels were made to separate the proteins of each fractionation run. One 10% gel and one 15% gel were placed into one vertical western blot gel apparatus and 1X SDS Page Running Buffer was added to first fill the space between the gels, then fill the outer container to the 2-gel line indicated on the container's wall. This was repeated for the second set of 10% and 15% gels. 7µL of Precision Plus Protein Standard Dual Color Ladder was loaded into the first lane of all four gels. 5µL of each chromatin-bound (CB) and soluble (S) protein fraction were loaded into the following lanes of both the 10% gel and the 15% gel in one gel apparatus. 10µL of each whole cell lysate fraction (WCL) were loaded in the lanes following the later in the second apparatus. It should be noted that the only exception to this loading order was the Nek2 verification experiment where all samples were able to fit on one gel, so only one 10% and one 15% were made and loaded. The samples were then run for 30 minutes at 90V to get samples through the initial stacking gel before the voltage was increased to 120V for about 90 minutes (only until the samples were about 0.5cm from the bottom of the gel).

Following electrophoresis, samples were transferred from their gels to a labeled 5.5 x 8.5 cm^2 nitrocellulose membrane in 1X Transfer Buffer with 20% methanol at 4°C for 90 minutes. Once transfer was complete, ladder markers were labeled (a line for blue lines and two dots for pink lines) and successful transfer was verified with a ponceau wash (just enough to cover the membrane) following three washes with water to remove remaining methanol. The 15% membrane was then cut with a razor blade horizontally immediately above the 25 kDa marker (lower pink/two dot line in ladder lane). Each 10% membrane and the upper halves of the 15% membrane were combined with 5mL of 5% milk-1X-TBST in a heat sealed baggie, while the lower halves of the 15% membrane were combined with 5mL of 5% BSA-1X-TBST a separate

heat sealed baggie. All membranes were placed on a rocker at room temperature to block for 45 minutes.

Following blocking, the 10% membranes were cut right above the 50kda marker and primary monoclonal antibodies for the Halo-tag of Suv420-Halo, for known soluble cytoplasmic proteins glyceraldehyde 3-phosphate dehydrogenase (GAPDH) and alpha tubulin (dm1α), and for known chromatin-bound protein histone 3 (H3) were diluted in either 5% milk+1X TBST or 5% BSA+1X TBST (1mL of milk for 1µL Halo, 1µL GPDH and 1µL dm1α each; 1mL of BSA for 5µL H3). Membranes were allowed to then rock at 4^{o}C overnight in new labeled heat-sealed bags with their respective primary monoclonal antibody mixtures (Halo in milk for upper halves of 10% membranes, GAPDH in milk for lower halves of 10% membranes, dm1α in milk for upper halves of 15% membranes, H3 in BSA for lower halves of 15% membranes). The following day (roughly 16 hours later), all membranes were washed three times in 1X TBST for 10 minutes each on a rocker in a small tupperware box (roughly 15 x 12 x 4 cm^3 - large enough to house the membranes and at least 10mL of liquid). Matching secondary antibodies (2µL of mouse secondary in 10mL of 5% milk + 1X TBST for Halo, GAPDH and dm1α; 2µL of rabbit secondary in 10mL of 5% BSA + 1X TBST for H3) were then added to their respective membranes and rocked for 75 minutes. Three more 1X TBST washes were then performed before all membranes were placed on a development cassette and 500µL of 1:1 prosignal pico:peroxide was added to each complete membrane (500µL per membrane, 1mL total for 2 membranes from 2 gels or 2mL total for 4 membranes from 4 gels). The prosignal pico:peroxide mixture was allowed to saturate the membrane for 30 seconds before all excess moisture was removed with clean kimtech wipes and the cassette was transferred to a developing room with an autoradiograph. Using autoradiography film sheets, six exposures of 1 second, 5 seconds, 10 seconds, 30 seconds, 1 minute and 5 minutes were taken and developed. Developed films were then labeled, scanned, and imported to ImageJ software for densitometry analysis.

ImageJ Densitometry and Statistical Calculations

Scanned, unaltered images of developed films were uploaded to ImageJ software where the entire row of bands for one protein was marked as Lane 1 and measured for band intensity. Bands in the resulting graph were then manually identified by adding line barriers that were equal distances apart along the x-axis. The area underneath each curve of the graph was then recorded as the raw measured band intensity. Normalized band intensities were then calculated by first dividing the band intensity of soluble fractions by the band intensity of their respective GAPDH or dm1α bands, and by dividing band intensity of chromatin-bound fractions by the band intensity of their respective H3 bands. These two ratios were then used to create the normalized ratio of chromatin-bound protein over soluble protein that was then used for statistical comparison (calculation of replicate averages, standard deviations of replicates and a double tailed Microsoft Excel T-test between conditions with $p<0.05$ for statistical significance) after at least three replicates of each experiment had been produced. If statistical significance was verified, the next experiment with a new set of opposing mutants was added to the next run.

Table of Methodology Materials & Reagents with Company Names and Catalog Numbers

Material/Reagent	Reagent Working Stock Volume & Concentration	Company Purchased From	Catalog/ Reference #
Cell Culture Materials			
10 cm^2 Tissue Culture Plates	N/A	Falcon Corning Brand	353003
Fetal Bovine Serum (FBS)	500mL	Sigma	12306C-500ML
Penicillin-Streptomycin (Penstrep)	100mL, 10000 U/mL	Gibco	15140-122
Dulbecco's Modified Eagle's Medium (Dmem)	500mL	GenClone (Genesee Scientific)	25-501
PES Bottled Vacuum Filter Unit	500mL, 0.2µm	Avantor	10040-436
Dimethyl sulfoxide (DMSO)	>99.5%	Sigma Aldrich	04540-500ML
Cryovials (Cell Freezer Tubes)	N/A	Simport Cryovial	T310-2A
Trypsin - EDTA solution (trypsin)	100mL, 0.25%	Sigma Aldrich	T4049-100ML
PBS	1X		
Kimtech Wipes	N/A	Kimberly-Clark Professional	34155
50mL conical tubes	N/A	Olympus Plastics	28-103
15mL conical tubes	N/A	Olympus Plastics	28-108
75cm^2 Tissue Culture Flasks, TC treated, Vented Cap, Sterile (T-75 flasks)	N/A	Fisher Scientific	FB012937
Drug Treatments			
Doxycycline	1mL, 2mg/mL	Sigma Aldrich	09891-1G
Nocodazole	1mL, 100mg/mL	Sigma	M1404
Rac CCT (Nek2i)	1mL, 10mM		250863
Calyculin A	1mL, 100mM	Millipore	028851-10UG
Cell Fractionation Materials			
Nonidet P-40 (NP40)	100mL, 10%	Sigma Chemical	N-3268
Bromophenol Blue	100%	Sigma Aldrich	114391-5G
2-mercaptoethanol (BME)	100g	Fisher Bioreagents	BP176-100
Tris Base	5kg	Fisher Bioreagents	BP152-5
Sodium dodecyl sulfate (SDS)	92.5-100.5%	Sigma Aldrich	L5750-50DG
Glycerol		Fisher Chemical	G33-1
Western Blot Gel Materials			
30% Acrylamide/0.8% Bisacrylamide	37.5:1 of 450mL	National Diagnostics	EC-890
Ammonium persulfate (APS)	10mL, 10%	Fisher Bioreagents	BP179-100
Tetramethylethylenediamine (TEMED)	99%	Sigma Aldrich	T9281-50ML
Tween 20		Research Products International	P20370-0.5
Glycine	5kg	Acros Organics	12007-0050

Material/Reagent	Reagent Working Stock Volume & Concentration	Company Purchased From	Catalog/ Reference #
Materials to Run Western Blot			
Methanol	100%	Fisher Chemical	A433P-4
Bovine Serum Albumin (BSA)	100%	Sigma Aldrich	A7030-500G
Powdered milk	N/A	That's Smart	G2853T74327
Nitrocellulose Membrane	0.45 micron, 30 cm x 3.5 m roll	ThermoScientific	88018
Glass Western Blot Plates	1.0mm	BioRad	
Western Blot Electrophoresis and Transfer Chamber	Mini Protein Tetra Cell	BioRad	552BR__
Precision Plus Protein Standard Dual Color Ladder	N/A	BioRad	161-0374
Acetic Acid	100%	Alfa Aesar	A10556
Ponceau			
Primary Anti-Halo Monoclonal Antibody	1mL, 1:1000	Promega	G921A
Primary Anti-GAPDH Monoclonal Antibody	50µL, 1:50	Protein Tech	60004-1g
Primary Anti-dm1α Monoclonal Antibody	1mL, 1:1000	Santa Cruz Biotechnology	SC-32293
Primary Anti-H3 Monoclonal Antibody	1mL, 1:1000	abCam	ab1791
ECL Anti-Mouse IgG, Horseradish Peroxidase linked whole Antibody (from sheep) (Mouse secondary antibody)	1mL, 1:1000	CiteAb	NA931V
ECL Anti-Rabbit IgG, Horseradish Peroxidase linked whole Antibody (from donkey) (Rabbit secondary antibody)	1mL, 1:1000	CiteAb	NA934V
Prosignal Pico: Peroxide	500mL kit	Prometheus Protein Biology Products	20-300B
Blue Devil Premium Sharp Autoradiography Film Sheets	N/A	Genesee Scientific	30-810
8" x 10" Autoradiography Cassette	N/A	Wolf X-ray Corporation NY	

The concentrations, company names and catalog numbers for all used reagents and materials for this project are listed by methodology category above. Please note that some materials repeat between categories but are not listed as so.

Results

Suv420 Association to Chromatin During Mitosis is Sensitive to Phosphorylation

To test if Suv420 localization on mitotic chromosomes is regulated by phosphorylation, I analyzed fractionated chromatin bound and soluble fractions from mitotic cells. To first confirm that Suv420-Halo expression could be induced via a 24h induction with doxycycline, I compared two groups of untreated RPE tetR Suv420-Halo cells, one which received doxycycline and one that did not receive doxycycline, and used western blotting approaches with a Halo-specific antibody to verify the doxy-dependent appearance of the Suv420-Halo. As seen in Figure 5 and in the Western blots in Appendix 2, cells that did not receive doxycycline had no Halo band, but did have GAPDH, alpha-tubulin and/or H3 bands. The GAPDH and alpha-tubulin, both soluble proteins, and Histone H3, a chromatin-bound protein, served as loading controls to verify that soluble and chromatin-bound fractions were correctly separated during fractionation.

I next compared fractionated samples from cells that were either untreated or treated with the phosphatase inhibitor CalcA. Using western blot analysis to quantify the amount of Suv420-Halo in each fraction, I determined that in untreated mitotic cells, Suv420-Halo is nearly evenly distributed between the chromatin bound and soluble fractions (average chromatin-bound to soluble ratio = 0.81; Figure 5A & Appendix 2, lanes 4 and 5). Treatment with CalcA, which is a broad inhibitor of phosphatase activity and is therefore expected to lock Suv420 in a phosphorylated state, resulted in a shift of Suv420-Halo shifting off of chromatin and into the soluble fraction (average chromatin-bound insoluble to soluble ratio = 0.33; Figure 5A, lanes 7 and 8), a 40.3% decrease from the untreated group. This result is consistent with the model whereby Suv420 localization to chromatin during mitosis is sensitive to phosphorylation.

Nek2 kinase activity limits Suv420 association with Chromatin

To next test if the Nek2 kinase may play a role in the phospho-regulation of Suv420 chromatin association, I compared the chromatin-bound and soluble fractions in untreated or Nek2i treated populations of cells. I found that treatment with Nek2i, which inhibits Nek2-dependent phosphorylation, resulted in an average chromatin-bound to soluble ratio of Suv420-Halo of 4.79, a 587.9% increase compared to the untreated group. This result suggests that Suv420 localization on chromatin is sensitive to Nek2-dependent phosphorylation and that Nek2 kinase activity normally acts to prevent Suv420 from binding stably to chromatin. A two tailed T-test of six replicates indicates that the changes in Suv420 localization based on Halo band intensity compared to the control group were statistically significant. The T-tests reported significance values of $P_{Nek2i} = 0.0189$ for Nek2i compared to untreated cells, and $P_{CalcA} = 0.0246$ for CalcA compared to untreated cells, verifying statistical significance ($P<0.05$) between the two treated cells and the untreated cells. Figure 5B provides a graphical representation of the recorded densitometry data and normalizing for sample to sample variation by dividing the densitometry value of the insoluble western blot band by its respective soluble band densitometry value.

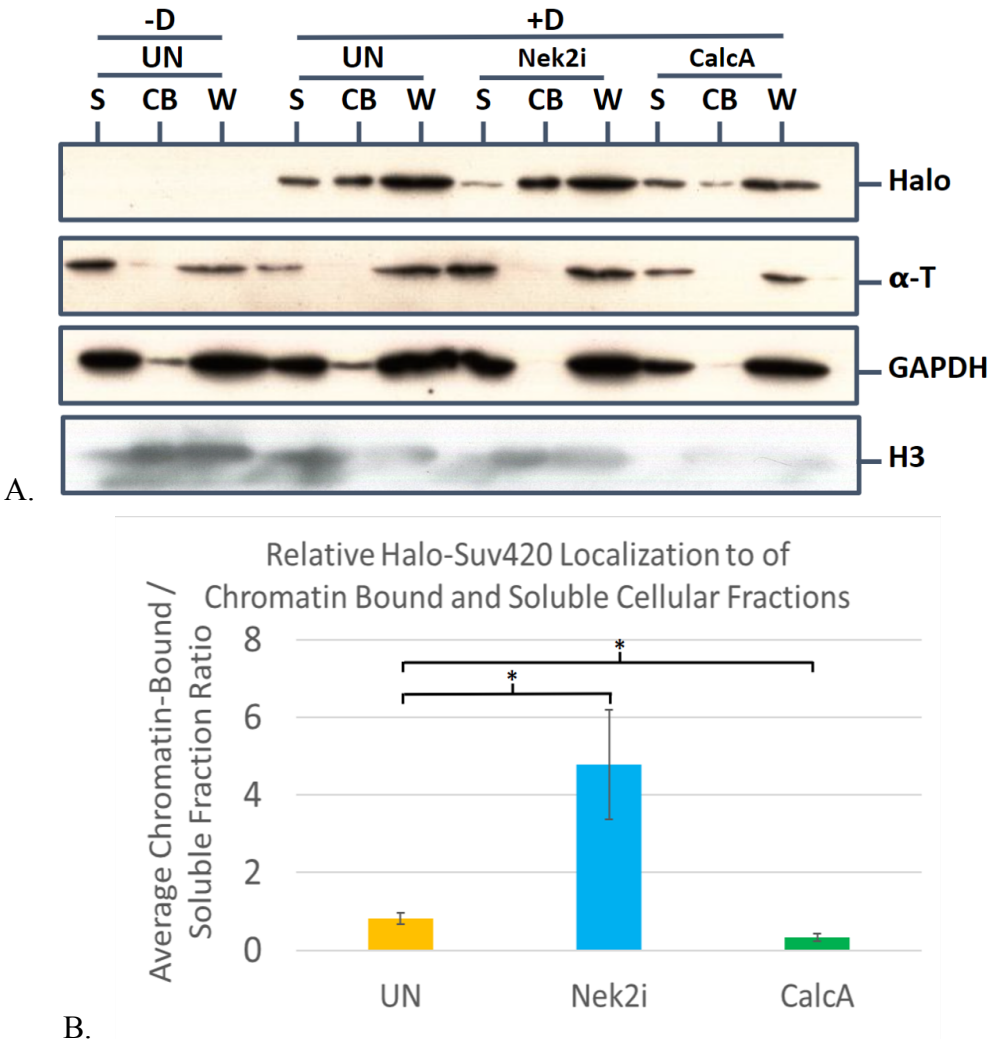

Figure 5: Nek2i and CalcA Found to be Significantly Different from Untreated RPE Cells.

A. Representative western blot results of small scale cellular fractionation verifying Nek2i and CalcA influence on Suv420 localization during mitosis. Two untreated groups of cells (UN) and two drug treated groups (Nek2i & CalcA) were probed for Halo, two known soluble proteins (S), alpha-tubulin (a-T) and GAPDH, and one chromatin-bound (CB) protein, Histone 3 (H3). One group of fractions (-D) did not receive doxycycline to induce Suv420-Halo expression while the other three groups did (+D). All cells received nocodazole.

B. ImageJ densitometry was performed on each Halo band in [A] and the average chromatin-bound over soluble cellular fraction ratios of 6 replicates was calculated and plotted in the graph above. Both Nek2i and CalcA average CB/S ratios were found to be significantly different (* $P<0.05$ is significant in a two tailed T-test: $P_{Nek2i}=0.0189$, $P_{CA}=0.0246$) from the untreated group. Error bars represent standard error.

differences in intensity between each treatment group. The western blot results of all six replicates (labeled by replicate number in the order of which they were performed) can be also found in Appendix 2 below. It should be also noted that although these results confirm that Suv420 localization to chromatin is dependent on successful Nek2 phosphorylation, it remains unknown whether this relationship is direct (Nek2 phosphorylating Suv420 as its substrate) or indirect (Nek2 phosphorylating an intermediate protein or proteins that then interact with Suv420 to change its chromatin association) and further experimentation is required to determine the two protein's relationship.

Mutation of predicted phosphorylation site Serine 20 of Suv420 does not perturb chromatin association

To further clarify the relationship between Suv420 and Nek2, the first of the four identified potential Nek2 phosphorylation sites, Serine 20, in Suv420's amino acid sequence was mutated to either an alanine or an aspartic acid to create phosphomimetic mutants, fractionated and analyzed by western blot. If Serine 20 was critical to Nek2 phosphorylation of Suv420, it was expected that mutating serine to alanine would alter the topical polarity of the Suv420 phosphorylation site and prevent phosphorylation, and that mutating serine to aspartic acid, a negatively charged amino acid, would prevent dephosphorylation of Suv420. Contrary to expectations, however, mutation of Serine 20 to an alanine, and mutation of Serine 20 to aspartic acid both resulted Suv420-Halo shifting off of chromatin and into the soluble fraction (average Suv420-Halo S20A insoluble to soluble ratio = 0.33, Figure 6A, and Appendix 3, lanes 3 and 4; average Suv420-Halo S20D insoluble to soluble ratio = 0.59, Figure 6A, and Appendix 3, lanes 5 and 6), a 61.37% and 72.43% decrease from the untreated group. However, as seen by the overlapping standard error bars in Figure 6B, neither mutant was found to have a statistically significant change in Suv420-Halo chromatin association in the mitotically arrested cells ($P_{\text{Suv420-Halo S20A}} = 0.3493$ & $P_{\text{Suv420-Halo S20D}} = 0.7432$) for the three analyzed replicates. It should be noted that, as seen in the representative Western blot in Figure 6B, more replicates with these mutants may reveal a subtle shift where the relative Halo-stained band intensities of both mutants appear to reflect a similar pattern to the Halo bands in the CalcA treated samples, although not nearly as pronounced (hence the quantitative conclusion of no significance for only three replicates with significant variation). More replicates of Suv420-Halo S20 should also generally be performed because although there may be no statistically significant difference from the untreated, wild-type Suv420-Halo cells, because significance was found between the untreated, wild-type Suv420-Halo cells and both the Nek2i and CalcA treated, wild-type Suv420-Halo cells, it is expected that both Suv420-Halo S20 mutants should show a significant difference from the two treated lines as well. However, this is not the case, with no P values comparing either treated group to either mutant being found to be below 0.05 for all three replicates ($P_{\text{Nek2i-Suv420-Halo S20A}} = 0.1923$, $P_{\text{Nek2i-Suv420-Halo S20D}} = 0.2032$,

A.

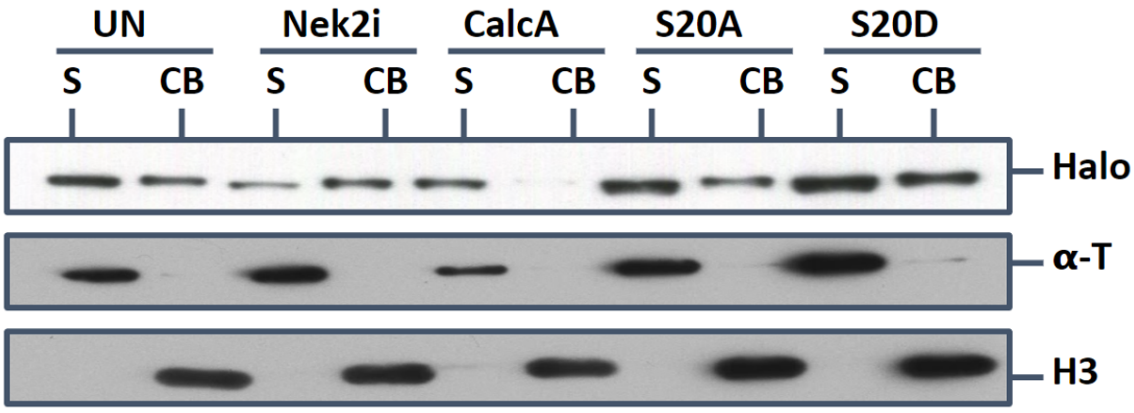

B.

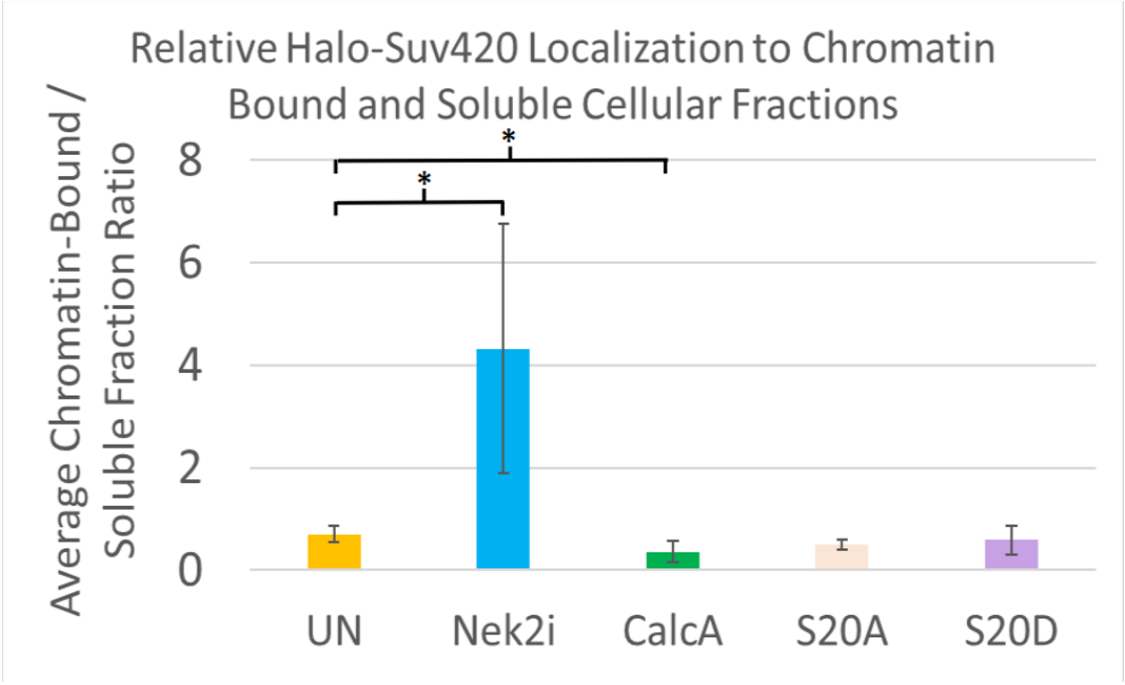

Figure 6: Suv420-Halo S20A and Suv420-Halo S20D Mutants Not Found to Significantly Change Suv420 Localization to Chromatin During Mitosis Compared to Untreated RPE Cells.

A. Representative western blot results of small scale cellular fractionation determining effect of mutation of Serine 20 on Suv420 localization during mitosis to reflect Nek2i and/or CalcA influence. Three untreated group of cells (one unmutated -UN- and two mutations -S20A & S20D-), and two drug treated groups (Nek2i & CalcA) were probed for Halo, one known soluble proteins (S) alpha-tubulin (a-T), and one chromatin-bound (CB) protein, Histone 3 (H3). All cells received doxycycline and nocodazole.

B. ImageJ densitometry was performed on each Halo band & the average average chromatin-bound over soluble cellular fraction ratios of 3 replicates with a mutation at Serine 20 was calculated and plotted in the graph on the right. Significance (*) is $p<0.05$ in two-tailed T-test for three replicates. Phosphomimetic mutation of Serine 20 to alanine (S20A) or aspartic acid (S20D) resulted in no significant change in Suv420 localization to chromatin during mitosis compared to wild type (WT) Suv420-Halo cells.

$P_{CalcAi\text{-}Suv420\text{-}Halo\ S20A} = 0.5783$, and $P_{CalcA\text{-}Suv420\text{-}Halo\ S20A} = 0.5449$). Like Appendix 2, all the western blot results of the three analyzed replicates containing the Suv420-Halo S20 mutants can be found in Appendix 3 below.

Discussion and Future Directions

As demonstrated in the results above, following treatment of RPE cells transformed with a Suv420-Halo tetracycline-inducible expression construct with phosphatase inhibitor Calyculin A, I found that Suv420 association to chromatin during mitosis is sensitive to phosphorylation . Additionally, treatment with a Nek2 kinase inhibitor that prevents Nek2-dependent phosphorylation further reveals that Nek2 kinase activity limits Suv420 association with chromatin. However, mutation of predicted Nek2 phosphorylation site Serine 20 of Suv420 does not perturb chromatin association.

To better understand the role of phosphorylation of Suv420 in its chromatin association, further experimentation should be performed with the three other predicted phosphorylation sites (T264, S355 & S449), mutating each site to create phosphomimetics and if no single site alone has significant effect on Suv420 localization to chromatin during mitosis, combinations of mutants can also be tested. Figure 7 below shows the western blot of one replicate performed with phosphomimetic mutants of Serine 355. As seen in the blot, although there appears to be no change in Suv420 localization to chromatin compared to untreated wild-type, S355D appears to alter the size of the Suv420-Halo protein, potentially by changing its phosphorylation state, resulting in the Halo bands of both soluble and insoluble fractions not traveling as far down the gel during electrophoresis compared to the other samples. Such alteration of Suv420-Halo could be verified by running a phos-tag gel followed by Western blotting [O'Donoghue & Smolenski, 2022].

Following identification of phosphomimetic mutants or combination of phosphomimetic mutants that significantly change Suv420 localization to chromatin during mitosis, these mutants should also then be treated with Nek2i and CalcA alongside wild type Suv420-Halo. It would be expected that any mutants that increase relative chromatin-bound fraction Suv420-Halo levels and decrease soluble fraction Suv420-Halo levels would revert to no significant difference with

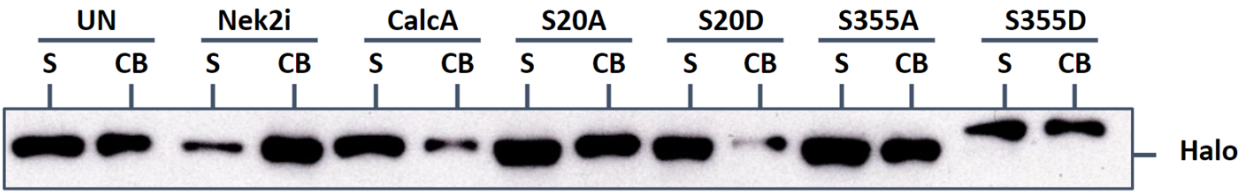

Figure 7: Western Blot of One Fractionation Replicate With Suv420-Halo S355 Phosphomimetic Mutants

The above is a preliminary western blot probing five untreated groups of cells (untreated wild type Suv420-Halo, & phosphomimetic mutants Suv420-Halo S20A, Suv420-Halo S20D, Suv420-Halo S355A & Suv420-Halo S355D) and two drug treated groups (Nek2i & CalcA) for Halo.

the addition of CalcA. The reverse would also be expected, with the addition of Nek2i to mutants that increase relative soluble fraction Suv420-Halo levels and decrease chromatin-bound fraction Suv420-Halo levels. Performing such experiments would allow for further verification of the previously observed trend in the mutants and would reconfirm Suv420's dependence on Nek2 phosphorylation.

Suv420-Halo Trends Should be Verified to Match Endogenous Suv420

Suv420-Halo plasmid was transfected into RPE cells under tetracycline control to enable more consistent and replicable experimentation, as well as allowing for the use of the Halo tag that is more efficiently bound to its respective monoclonal antibody for Western blotting. However, analysis of the Halo bands during densitometry makes the assumption that the Suv420-Halo plasmid is being expressed in the same manner and to the same levels as endogenous Suv420, and that the Halo tag has no impact on Suv420's methyltransferase activity or the protein's localization in the cell. To verify this, all of the membranes that have been probed for Halo can also be stripped and reprobed for endogenous Suv420. Ensuring that the ratio of Suv420 between the soluble and insoluble fractions of the endogenous Suv420 bands matches the ratio of the Halo bands would confirm that this assumption is true.

In addition to probing for endogenous Suv420, other proteins whose localization to chromatin is also known to be affected directly by Suv420's localization to chromatin during mitosis, particularly Aurora B can be probed for. If Aurora B bands on the western blot membranes have the opposite ratio of soluble Aurora B to chromatin-bound Aurora B compared to the ratio of the Halo and/or endogenous Suv420 bands, which is expected based on the finding that increased Suv420 localization to the pericentromeres during mitosis inhibits Aurora B localization to the centromeres [Herlihy et al., 2021], probing for Aurora B would thus be expected to confirm three assumptions. It would reinforce if Suv420-Halo does not interfere with endogenous Suv420's activity and/or is accurately reflective of it, reinforce if endogenous Suv420 is sensitive to Nek2 phosphorylation, and reconfirm the relationship that has been found between Aurora B and Suv420 by Herlihy et al. [2021].

Conclusions and Broader Implications

Having confirmed Suv420's sensitivity to Nek2 phosphorylation state, the larger question to be asked next is how such data can be applied to the field of cancer biology and to the creation of cancer therapies and treatments. As previously mentioned, misregulation of either Suv420 or Nek2 has been linked to the development and progression of a number of cancers [Wu et al., 2018; Shamloo & Usluer, 2019; Shah et al., 2022; Xie & Weiskirchen, 2020]. However, regulation of Suv420 expression and activity are still relatively unknown within the literature despite the large majority examining changes in Suv420 expression as drivers of cancer development and progression within the cell. Most studies find that Suv420 is either overexpressed/overactive and is silencing critical tumor suppressor genes, or that Suv420 is inactivated, resulting in overall loss of H4K20 trimethylation at the telomeres and on many

oncogenic genes [Gabellini & Pedrotti, 2022]. The data of these experiments partially answers the question of Suv420 regulation during mitosis and it suggests that there may be a more complicated story to cancer progression involving Suv420. It is possible that some cancers that have been found to have misregulated Suv420 could be driven not by inactivation or overexpression of the methyltransferase itself, but by a failure in the proper regulation, particularly by Nek2 during mitosis. That failure in regulation of localization during mitosis may then result in such a significant genotypic alteration that the cell is able to further progress to a more cancerous and malignant state from improper chromosome segregation. Given that the data above suggests that misregulation of Suv420 may be the result of Nek2 misregulation (particularly the upregulation of Nek2 known to have oncogenic effects [Shah et al, 2022; Xie & Weiskirchen, 2020]), it is possible that disruption of Suv420 activity at the centromeres during mitosis via inhibition of Nek2 phosphorylation may enable restoration of proper regulation of microtubule-kinetochore attachment dynamics to reduce the progression of cancer that can occur as a result of failed mitotic fidelity. Nek2 may thus serve as a potent target of therapy in cancers where Suv420 has been found to be misregulated. Likewise, in cancers where Nek2 is acting oncogenically, inhibition of Suv420 localization to centromeres during mitosis may serve as a potential target for cancer treatment in combination with other Nek2 substrates to stop the downstream effects of Nek2 upregulation, stopping the drive to ignore the spindle assembly checkpoint requirements and to continue through the cell cycle. In addition to application of direct cancer treatment and therapy targets, given that both proteins can be found at a number of different critical biochemical pathways that generally must be maintained or upregulated by cancer cells to continue viable division, both proteins may also serve as strong indicators for tracking the development of cancer onset and malignancy. Cancers that have either Suv420 or Nek2 misregulated could be better combated by improving cancer detection using the localization of Suv420 within a mitotic cancer cell or Nek2 phosphorylation activity within cancer patient's samples as a biomarker for tracking progression.

However, to determine how either protein can be used either as a cancer therapeutic target or as a biomarker to track cancer progression, more research must be done to further clarify the relationship between Suv420 and Nek2, as well as to understand how the activities of both proteins together have changed within the context of cancer. Additionally, the data analyzed is limited by the lack of completely functional controls due to issues with western blot transfer from gel to membrane and changing monoclonal antibody strength. Use of 20% methanol in the 1X Transfer buffer and allowing for a minimum of 90 minutes at 90V was critical for complete protein transfer from gel to membrane. Use of the correct concentration of primary antibody for each probed protein was also critical for a more robust analysis, but was unable to be accomplished for enough replicates to perform in this experiment. This can be seen in Figure 4 in the Appendix of Figures, where the Halo bands of each experiment are clear, but the GAPDH, alpha-tubulin and histone 3 controls are not consistently present, nor is the inclusion of a whole cell lysate. Ideally, the most accurate measure of Suv420 localization to chromatin would include analysis of relative band intensity of the known soluble and insoluble proteins that were probed

(GAPDH, alpha-tubulin and histone 3). By comparing the Halo band intensities between soluble and insoluble chromatin bound fractions after also comparing each fraction to its respective known soluble or insoluble band intensities, a more robust analysis of this experiment's results could be performed.

In conclusion, based on the results of this project, multiple replicates verify that Suv420 association with chromatin during mitosis is dependent on Nek2 phosphorylation. Inhibition of Nek2 phosphorylation (via RacCCT's binding to Nek2's catalytic pocket) increased Suv420 localization to chromatin while inhibition of dephosphorylation by CalcA decreased Suv420 localization to chromatin. However, the next questions of how Nek2 phosphorylation specifically regulates Suv420 localization and then how changing the activity of either protein specifically affects correct chromosome segregation of the cell during mitosis remains to be seen. Testing phosphomimetic mutants of Suv420, both with and without treatment by either Nek2i or CalcA, and probing for endogenous Suv420 and Aurora B would be necessary to answering these questions and are therefore highly recommended as the first experiments to conduct following this project. Beyond these specific experiments though, more research in general examining Suv420 and Nek2's role in cancer development and progression is also highly recommended in order to determine how either protein may be utilized as a potent target for specialized cancer therapy.

Works Cited

Alberts B, Johnson A, Lewis J, et al. Molecular Biology of the Cell. 4th edition. New York: Garland Science; 2002. An Overview of the Cell Cycle. Available from: https://www.ncbi.nlm.nih.gov/books/NBK26869/

Beswick, R. Ambrose, H. Wagner, S. 2006. Nocodazole, a microtubule depolymerising agent, induces apoptosis of chronic lymphocytic leukaemia cells associated with changes in Bcl-2 phosphorylation and expression. Leukemia Research, 30(4), 427 - 436. https://doi.org/10.1016/j.leukres.2005.08.009

Bethesda, M. D. (2022) PDQ Screening and Prevention Editorial Board. Cancer Prevention Overview (PDQ®): Health Professional Version. In: PDQ Cancer Information Summaries [Internet]. National Cancer Institute (US). https://www.ncbi.nlm.nih.gov/books/NBK66016/

Binarová, P., & Tuszynski, J. (2019). Tubulin: Structure, Functions and Roles in Disease. Cells, 8(10), 1294. https://doi.org/10.3390/cells8101294

Broad, A. J. DeLuca, K. F. DeLuca, J. G. (2020). Aurora B kinase is recruited to multiple discrete kinetochore and centromere regions in human cells. Journal of Cell Biology 2, 219(3), e201905144. https://doi.org/10.1083/jcb.201905144

Bromberg, K., Mitchell, T., Upadhyay, A. et al. The SUV4-20 inhibitor A-196 verifies a role for epigenetics in genomic integrity. Nat Chem Biol 13, 317–324 (2017). https://doi.org/10.1038/nchembio.2282

Chow, A. Y. (2010) Cell Cycle Control by Oncogenes and Tumor Suppressors: Driving the Transformation of Normal Cells into Cancerous Cells. Nature Education 3(9):7

Ciferri, C., De Luca, J., Monzani, S., Ferrari, K. J., Ristic, D., Wyman, C., Stark, H., Kilmartin, J., Salmon, E. D., & Musacchio, A. (2005). Architecture of the human ndc80-hec1 complex, a critical constituent of the outer kinetochore. The Journal of biological chemistry, 280(32), 29088–29095. https://doi.org/10.1074/jbc.M504070200

Cooper GM. The Cell: A Molecular Approach. 2nd edition. Sunderland (MA): Sinauer Associates; 2000. The Development and Causes of Cancer. Available from: https://www.ncbi.nlm.nih.gov/books/NBK9963/

Curtis, N. Ruda, G. Brennan, P. Bolanos-Garcis, V. (2020). Deregulation of Chromosome Segregation and Cancer. Ann. Rev. Cancer Biol. 4(1), 257-278. https://doi.org/10.1146/annurev-cancerbio-030419-033541

Gordon, D., Resio, B. & Pellman, D. (2012) Causes and consequences of aneuploidy in cancer. Nat Rev Genet 13, 189–203. https://doi.org/10.1038/nrg3123

Gupta, A., Hunt, C. R., Chakraborty, S., Pandita, R. K., Yordy, J., Ramnarain, D. B., Horikoshi, N., & Pandita, T. K. (2014). Role of 53BP1 in the regulation of DNA double-strand break repair pathway choice. Radiation research, 181(1), 1–8. https://doi.org/10.1667/RR13572.1

Herlihy, C. P., Hahn, S., Hermance, N. M., Crowley, E. A., & Manning, A. L. (2021). Suv420 enrichment at the centromere limits Aurora B localization and function. Journal of cell

science, 134(15), jcs249763. https://doi.org/10.1242/jcs.249763

Herwig, S., & Strauss, M. (1997). The retinoblastoma protein: a master regulator of cell cycle, differentiation and apoptosis. European journal of biochemistry, 246(3), 581–601. https://doi.org/10.1111/j.1432-1033.1997.t01-2-00581.x

Hindriksen, S., Lens, S. M. A., & Hadders, M. A. (2017). The Ins and Outs of Aurora B Inner Centromere Localization. Frontiers in cell and developmental biology, 5, 112. https://doi.org/10.3389/fcell.2017.00112

Hinshaw, S. M., & Harrison, S. C. (2018). Kinetochore Function from the Bottom Up. Trends in cell biology, 28(1), 22–33. https://doi.org/10.1016/j.tcb.2017.09.002

Hu, J., Cao, J., Topatana, W. et al. Targeting mutant p53 for cancer therapy: direct and indirect strategies. J Hematol Oncol 14, 157 (2021). https://doi.org/10.1186/s13045-021-01169-0

Invitrogen Corporation. (2023). Gateway Technology User Guide To Clone DNA Sequences for Functional Analysis and Expression in Multiple Systems. Gateway Technology User Guide. Retrieved April 25, 2023, from https://www.thermofisher.com/document-connect/document-connect.html?url=https://assets.thermofisher.com/TFS-Assets%2FLSG%2Fmanuals%2Fgatewayman.pdf

Innocenti, P., Cheung, K. M., Solanki, S., Mas-Droux, C., Rowan, F., Yeoh, S., Boxall, K., Westlake, M., Pickard, L., Hardy, T., Baxter, J. E., Aherne, G. W., Bayliss, R., Fry, A. M., & Hoelder, S. (2012). Design of potent and selective hybrid inhibitors of the mitotic kinase Nek2: structure-activity relationship, structural biology, and cellular activity. Journal of medicinal chemistry, 55(7), 3228–3241. https://doi.org/10.1021/jm201683b

Ishihara, H., Martin, B. L., Brautigan, D. L., Karaki, H., Ozaki, H., Kato, Y., Fusetani, N., Watabe, S., Hashimoto, K., & Uemura, D. (1989). Calyculin A and okadaic acid: inhibitors of protein phosphatase activity. Biochemical and biophysical research communications, 159(3), 871–877. https://doi.org/10.1016/0006-291x(89)92189-x

Islami, F. Ward, E. M. Sung, H. Cronin, K. A. Tangka, F. K. L. Sherman, R. L. Zhao, J. Anderson, R. N. Henley, S. J. Yabroff, K. R. Jemal, A. Benard V. B. Annual report to the nation on the status of cancer, part 1: national cancer statistics, Journal of the National Cancer Institute, Volume 113, Issue 12, December 2021, Pages 1648–1669, https://doi.org/10.1093/jnci/djab131

Janssen, A., Colmenares, S. U., & Karpen, G. H. (2018). Heterochromatin: Guardian of the Genome. Annual review of cell and developmental biology, 34, 265–288. https://doi.org/10.1146/annurev-cellbio-100617-062653

Kumar, M., Michael, S., Alvarado-Valverde, J., Mészáros, B., Sámano-Sánchez, H., Zeke, A., Dobson, L., Lazar, T., Örd, M., Nagpal, A., Farahi, N., Käser, M., Kraleti, R., Davey, N. E., Pancsa, R., Chemes, L. B., & Gibson, T. J. (2021). The eukaryotic linear motif resource: 2022 release. Nucleic Acids Research, 50(D1), D497–D508. https://doi.org/10.1093/nar/gkab975

Lampson, M. A., Renduchitala, K., Khodjakov, A., & Kapoor, T. M. (2004). Correcting improper

chromosome-spindle attachments during cell division. Nature cell biology, 6(3), 232–237. https://doi.org/10.1038/ncb1102

Liang, C., Zhang, Z., Chen, Q., Yan, H., Zhang, M., Zhou, L., Xu, J., Lu, W., & Wang, F. (2020). Centromere-localized Aurora B kinase is required for the fidelity of chromosome segregation. The Journal of cell biology, 219(2), e201907092. https://doi.org/10.1083/jcb.201907092

McIntosh J. R. (2016). Mitosis. Cold Spring Harbor perspectives in biology, 8(9), a023218. https://doi.org/10.1101/cshperspect.a023218

Mulder, N. J., & Apweiler, R. (2002). Tools and resources for identifying protein families, domains and motifs. Genome biology, 3(1), REVIEWS2001. https://doi.org/10.1186/gb-2001-3-1-reviews2001

Musacchio, A., & Desai, A. (2017). A Molecular View of Kinetochore Assembly and Function. Biology, 6(1), 5. https://doi.org/10.3390/biology6010005

Musacchio, A., Salmon, E. (2007)The spindle-assembly checkpoint in space and time. Nat Rev Mol Cell Biol 8, 379–393. https://doi.org/10.1038/nrm2163

O'Donoghue, L., & Smolenski, A. (2022). Analysis of protein phosphorylation using Phos-tag gels. Journal of proteomics, 259, 104558. https://doi.org/10.1016/j.jprot.2022.104558

Ong, J. Y., & Torres, J. Z. (2019). Dissecting the mechanisms of cell division. The Journal of biological chemistry, 294(30), 11382–11390. https://doi.org/10.1074/jbc.AW119.008149

Sachdeva, U. M., & O'Brien, J. M. (2012). Understanding pRb: toward the necessary development of targeted treatments for retinoblastoma. The Journal of clinical investigation, 122(2), 425–434. https://doi.org/10.1172/JCI57114

Shamloo, B., & Usluer, S. (2019). p21 in Cancer Research. Cancers, 11(8), 1178. https://doi.org/10.3390/cancers11081178

Shah, D, Joshi, M, Patel, BM. Role of NIMA-related kinase 2 in lung cancer: Mechanisms and therapeutic prospects. Fundam Clin Pharmacol. 2022; 36(5): 766- 776. https://doi.org/10.1111/fcp.12777

Shi, L., Wen, H., & Shi, X. (2017). The Histone Variant H3.3 in Transcriptional Regulation and Human Disease. Journal of molecular biology, 429(13), 1934–1945. https://doi.org/10.1016/j.jmb.2016.11.019

Southall, S. M., Cronin, N. B., & Wilson, J. R. (2014). A novel route to product specificity in the Suv4-20 family of histone H4K20 methyltransferases. Nucleic acids research, 42(1), 661–671. https://doi.org/10.1093/nar/gkt776

Taylor, A. M., Shih, J., Ha, G., Gao, G. F., Zhang, X., Berger, A. C., Schumacher, S. E., Wang, C., Hu, H., Liu, J., Lazar, A. J., Cancer Genome Atlas Research Network, Cherniack, A. D., Beroukhim, R., & Meyerson, M. (2018). Genomic and Functional Approaches to Understanding Cancer Aneuploidy. Cancer cell, 33(4), 676–689.e3. https://doi.org/10.1016/j.ccell.2018.03.007

United States Census Bureau [US Census Bureau] https://www.census.gov/popclock/

Wang, T., Holt, M.V. & Young, N.L. The histone H4 proteoform dynamics in response to

SUV4-20 inhibition reveals single molecule mechanisms of inhibitor resistance. Epigenetics & Chromatin 11, 29 (2018). https://doi.org/10.1186/s13072-018-0198-9

Welburn, J. P., Vleugel, M., Liu, D., Yates, J. R., 3rd, Lampson, M. A., Fukagawa, T., & Cheeseman, I. M. (2010). Aurora B phosphorylates spatially distinct targets to differentially regulate the kinetochore-microtubule interface. Molecular cell, 38(3), 383–392. https://doi.org/10.1016/j.molcel.2010.02.034

Wu, Y., Wang, Y., Liu, M., Nie, M., Wang, Y., Deng, Y., Yao, B., Gui, T., Li, X., Ma, L., Guo, C., Ma, C., Ju, J., & Zhao, Q. (2018). Suv4-20h1 promotes G1 to S phase transition by downregulating p21WAF1/CIP1 expression in chronic myeloid leukemia K562 cells. Oncology letters, 15(5), 6123–6130. https://doi.org/10.3892/ol.2018.8092

Zhang, J. Y., Zhang, F., Hong, C. Q., Giuliano, A. E., Cui, X. J., Zhou, G. J., Zhang, G. J., & Cui, Y. K. (2015). Critical protein GAPDH and its regulatory mechanisms in cancer cells. Cancer biology & medicine, 12(1), 10–22. https://doi.org/10.7497/j.issn.2095-3941.2014.0019

Zhang, Y. Zheng, P. (2022). NEK2 inactivates the Hippo pathway to advance the proliferation of cervical cancer cells by cooperating with STRIPAK complexes, Cancer Letters, Volume 549, 2022, 215917, ISSN 0304-3835, https://doi.org/10.1016/j.canlet.2022.215917.

Zhou, M., Li, Y., Lin, S., Chen, Y., Qian, Y., Zhao, Z., & Fan, H. (2019). H3K9me3, H3K36me3, and H4K20me3 Expression Correlates with Patient Outcome in Esophageal Squamous Cell Carcinoma as Epigenetic Markers. Digestive diseases and sciences, 64(8), 2147–2157. https://doi.org/10.1007/s10620-019-05529-2

Appendix of Tables & Figures

Appendix 1: Recipes of All Used Reagents

Reagent	Reagent Components	Special Instructions
Cell Culture Materials		
Cell Culture Media (500mL)	500mL Dmem 50mL FBS 5mL Penstrep	Combine all and filter via 500mL 0.2µm sterile PES Filter unit. Store at 4°C
Fractionation Materials		
Hypotonic Buffer (50mL)	500µL 1M HEPES (pH 7.9) 500µL 1M KCl 20µL 500mM EDTA 50µL 500mM EGTA 48.93mL dH2O	Store at 4°C
10% NP40 (250mL)	25mL 100% NP40 225mL dH_2O	
4X Sample Lysis Buffer (10mL)	2.5mL of 1M Tris, pH 6.8 (250mM) 0.8g SDS (8%) 4mL of 100% glycerol (40%) 0.002g bromophenol blue (0.02%) 2.9mL dH2O	Use in 2ml aliquots, add 60µL BME (2-mercaptoethanol) per mL of stock to aliquots only. Store at 4°C
1X Sample Buffer (1mL)	250µL 4X Sample Lysis Buffer 750µL hypotonic buffer	Store at -20°C
Western Blot Materials		
10X SDS Page Buffer (1L)	500ml of dH_2O 30.25g Tris Base. 144 g Glycine. 10 g SDS.	Once all components are combined and the solution has been mixed to clarity, add dH_2O until the volume is 1L.
1X SDS Page Buffer (1L)	100mL 10X SDS Page Buffer 900mL dH_2O	
10X Transfer Buffer (1L)	500ml of dH_2O	Once all components

	144.2 g Glycine. 30.2g Tris Base.	are combined and the solution has been mixed to clarity, add dH_2O until the volume is 1L.
1X Transfer Buffer w/ 20% methanol (2L)	200mL 10X Transfer Buffer 400 mL methanol 1.4L dH_2O	Store overnight at 4°C
10X TBST (1L)	500ml of dH_2O 24.2g Tris Base. 84g NaCl Use HCl to bring the pH to 7.4 10mL of Tween20.	Once all components are combined and the solution has been mixed to clarity, add dH_2O until the volume is 1L.
1X TBST (1L)	100mL 10X TBST 900mL dH_2O	
5% milk + 1X TBST (50mL)	2.5g powdered milk 50mL 1X TBST	Can be stored for only a few days at 4°C. Best to make fresh
5% BSA + 1X TBST (25mL)	1.25g BSA 25mL 1X TBST	Can be stored for only a few days at 4°C. Best to make fresh
Primary GAPDH Antibody Stock (1:50, 1mL)	1µL GAPDH stock 5µL dmso 44µL 1X TBST	Store at -20°C
Primary H3 Antibody Stock (1:1000, 1mL)	1µL H3 stock 100µL dmso 899µL 1X TBST	Store at -20°C

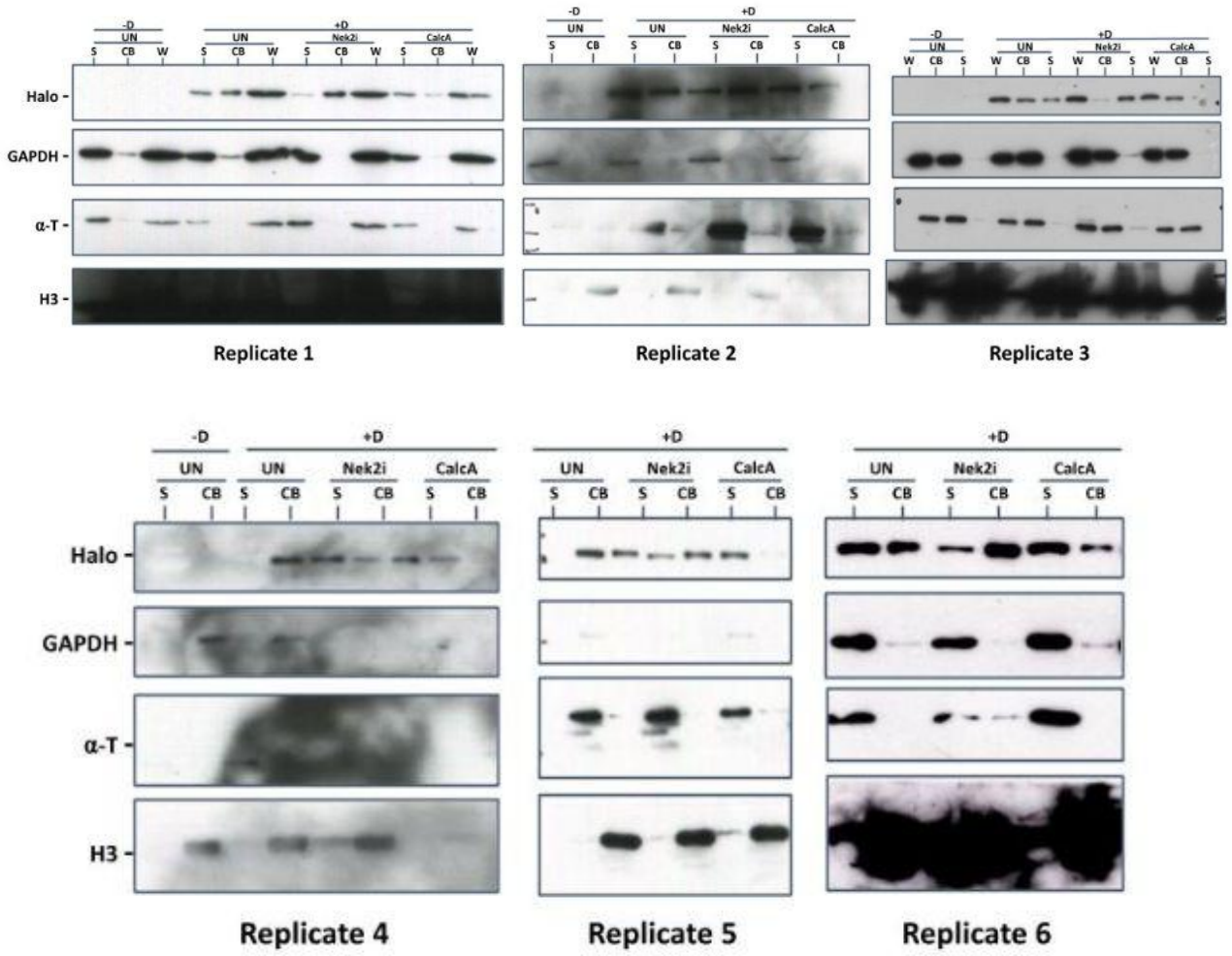

Appendix 2: Western Blot of Six Fractionation Replicates of Suv420-Halo Wild Type RPE Cell Lines

Representative Western blot results of all small scale cellular fractionation replicates verifying Nek2i and CalcA influence on Suv420 localization during mitosis. Two untreated groups of cells (UN) and two drug treated groups (Nek2i & CalcA) were probed for Halo, two known soluble proteins (S), alpha-tubulin (a-T) and GAPDH, and one chromatin-bound (CB) protein, Histone 3 (H3). Groups of fractions labeled -D did not receive doxycycline to induce Suv420-Halo expression while the other groups labeled +D received doxycycline. All cells received nocodazole.

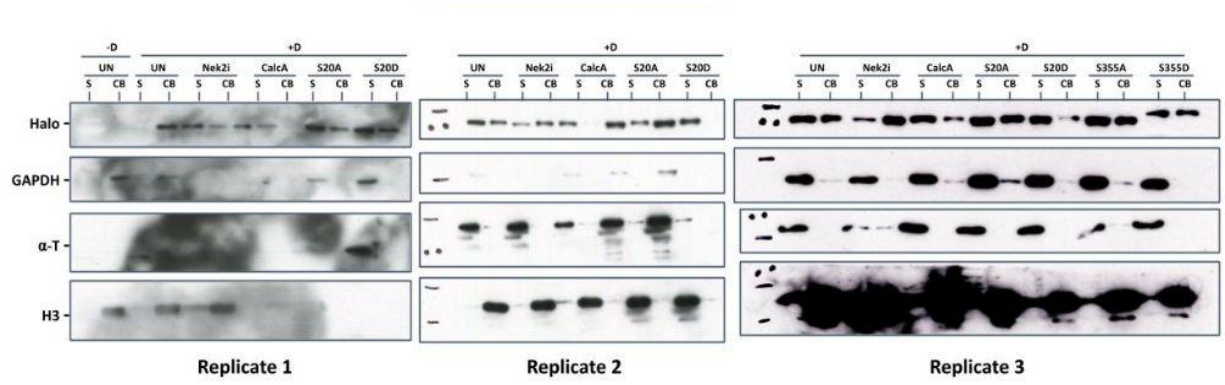

Appendix 3: Western Blot of Three Fractionation Replicates of Suv420-Halo RPE Cell Lines With S20 Phosphomimetic Mutants

All Western blot results of small scale cellular fractionation testing influence on Suv420 localization during mitosis by creating phosphomimetic mutations at Serine 20 of Suv420-Halo. Three untreated group of cells (one unmutated -UN- and two mutations -S20A & S20D-), and two drug treated groups (Nek2i & CalcA) were probed for Halo, two known soluble proteins (S), alpha-tubulin (a-T) and GAPDH, and one chromatin-bound (CB) protein, Histone 3 (H3). All cells received doxycycline and nocodazole.